Secure Communications for UAV Relay Networks: A MPC-Based Trajectory Tracking Approach

Shizhan Lan *, Lei Zhong , Bin Tan , Yeyu Liang , Shan Chen , Hanghang Xie

Posted Date: 24 February 2025

doi: 10.20944/preprints202502.1810.v1

Keywords: UAV; MPC; trajectory design; power allocation

Article

Secure Communications for UAV Relay Networks: A MPC-Based Trajectory Tracking Approach

Shizhan Lan [1,2,*], Lei Zhong [2], Bin Tan [2], Yeyu Liang [2], Shan Chen [2] and Hanghang Xie [2]

[1] School of Software Engineering, South China University of Technology, Guangzhou 510006, China
[2] China Mobile Guangxi Co., Ltd, Nanning, 530012, China
* Correspondence: lanshizhan@gx.chinamobile.com

Abstract: Unmanned aerial vehicles (UAVs) have emerged as a promising solution to enhance communication networks, especially in scenarios where traditional infrastructure is impractical or unavailable. However, the reliance on line-of-sight (LoS) channels in UAV-assisted relay networks introduces significant security vulnerabilities. This paper proposes a novel framework that jointly optimizes transmit power and UAV trajectory to achieve secure communications in such networks. To enhance system performance against environmental uncertainties, we employ a model predictive control (MPC)-based approach, which allows for real-time adaptive control of the UAV's trajectory by considering future states and disturbances. This approach significantly improves the network's resilience to dynamic environments and potential eavesdropping threats. Simulation results show that the proposed joint optimization of power allocation and trajectory design not only enhances communication security but also demonstrates the effectiveness of the MPC framework in real-time trajectory tracking, ensuring robust performance under varying environmental conditions.

Keywords: UAV; MPC; trajectory design; power allocation.

1. Introduction

Unmanned aerial vehicles (UAVs) have garnered significant attention in recent years due to their potential to revolutionize various sectors, including communication, surveillance, and transportation [1–5]. Among the various applications, UAVs are increasingly being considered as relays in communication networks [6–8]. The ability of UAVs to operate at different altitudes and provide coverage over vast areas makes them ideal candidates for communication relays in situations where traditional infrastructure is impractical or unavailable [9]. In [10], an energy efficiency maximization algorithm for UAV relay with a circular trajectory is proposed, where the problem focuses on optimizing speed and load factor to balance power consumption and communication capacity. Zeng *et al.* [11] explore throughput maximization for UAV relays with a rectilinear trajectory, optimizing both power allocation and trajectory design to enhance performance under mobility constraints and information-causality conditions. While the concept of using UAV relays with a fixed location or on a fixed trajectory has been explored in several studies, there is a growing interest in mobile UAV relays, which provide enhanced flexibility and performance over their stationary counterparts [12]. A mobile UAV relay can follow dynamic paths and adjust its position to optimize communication performance, thereby improving coverage and reducing the likelihood of interference or signal blockage [13–16].

However, the line-of-sight (LoS) channel between UAVs and ground stations introduces significant security risks that must be addressed [13,17–19]. While UAV-based relay networks offer high throughput and low latency, their reliance on LoS paths can expose the system to various security vulnerabilities, including unauthorized interception of signals and cyber-attacks [20–22]. The security of UAV-assisted communication has been studied in [19,23–25], focusing on physical layer security (PLS) techniques. The authors in [23,24] optimized UAV relays by designing power allocation for secure communications. In [25], the authors improved secrecy rates by exploiting UAV mobility, while Wu *et al.* [19] proposed real-time UAV trajectory design in integrated sensing and communication

 doi:10.20944/preprints202502.1810.v1

(ISAC) systems, using an extended Kalman filtering (EKF)-based method for tracking to maximize secrecy rate.

Beyond the security challenges in UAV relay networks, the deployment of mobile UAVs also presents additional complexities, such as the need for accurate trajectory planning and control to ensure that communication links remain stable and reliable [26–28]. Current methods for mobile UAV relay systems often suffer from limitations in trajectory tracking accuracy and real-time adaptability, highlighting the need for more sophisticated control approaches [29–32]. Linear quadratic regulator (LQR)-based has been widely used for controlling UAVs in stationary applications, where it optimizes the control inputs based on a quadratic cost function. For example, an innovative method for adjusting the weighting matrices in linear quadratic LQR and LQR-proportional integral (PI) controllers significantly enhanced the robustness and tracking capabilities of quadrotor stabilization [33]. However, when considering dynamic scenarios, such as mobile UAV relays, the more advanced model predicted control (MPC) approach becomes critical. MPC allows for real-time optimization of the UAV's trajectory, accounting for both the current state and future predictions, which is particularly important in environments with changing communication requirements or constraints [34,35]. While existing studies focus on either secure communication or trajectory control in UAV relay networks, their integration remains unexplored. To the best of our knowledge, this is the first work jointly optimizes security and trajectory tracking using MPC-based approach. This paper addresses this gap by proposing a framework that ensures both secure and efficient UAV relay operations. The main contributions of this work are summarized as follows:

- We propose a novel framework that jointly optimizes the transmit power and UAV trajectory, aiming to enhance the security of UAV-assisted relay networks, which ensures a balance between efficient communication and robust security against potential eavesdropping. To address the resultant non-convex secrecy rate maximization problem, we first divide the original problem into two sub-problems that optimize the UAV transmit power and trajectory separately by leveraging the successive convex approximation (SCA) techniques.
- We employ a MPC-based approach to adaptively control the UAV's trajectory that improves secure communication. By considering future states and disturbances, the MPC method optimizes the control input termed velocity in each time slot, enabling the UAV to follow the trajectory efficiently while adapting to practical constraints and disturbances, enhancing the system's resilience to dynamic environmental changes and security threats.
- Extensive simulation results demonstrate the effectiveness of the proposed framework. The joint optimization of power allocation and trajectory design leads to significant improvements in communication security, while the MPC-based path tracking ensures robust performance, highlighting the superiority of our approach compared to traditional methods, particularly in dynamic and uncertain environments.

The remainder of this paper is structured as follows: Section 2 presents a detailed description of the proposed UAV relay network system, including both the secure communication model and the trajectory control model. Next, Section 3 formulates and solves the UAV power allocation and trajectory design problem, followed by the MPC-based trajectory tracking discussed in Section 4. Section 5 presents the simulation results. Finally, Section 6 offers the conclusion of the paper.

Notations: Bold lowercase and uppercase letters, such as $\mathbf{a}$ and $\mathbf{A}$, represent vectors and matrices, respectively. $\mathbb{R}^M$ denotes the M-dimensional real-valued column vectors. $(\cdot)^T$ and $(\cdot)^{-1}$ denote the transposition and inverse operation, respectively. $\|\cdot\|$ indicates the ℓ_2-norm of a matrix. $\mathcal{N}(a, b)$ is employed to represent a Gaussian distribution of mean a and variance b. Additionally, $\text{diag}(\cdot)$ represents a diagonal matrix, and $\mathbf{I}_M$ refers to the $M \times M$ identity matrix.

2. System Model

As depicted in Figure 1, we consider a downlink communication scenario, where a base station (BS) is employed to serve a ground user (Bob) in the presence of an eavesdropper (Eve), with both out

 doi:10.20944/preprints202502.1810.v1

of the coverage of BS. Consequently, we assume that the transmission between the BS and UAV is in the absence of eavesdropping. A single-antenna UAV is utilized as an amplify-and-forward (AF) relay to assist the success of downlink transmission. For ease of exposition, we focus on a total duration of length T, which is further split into N time slots with the duration of each time slot Δt. Notably, the value of Δt should be small enough, enabling the UAV location within each time slot to approximately remain unchanged. During downlink transmission, the UAV dynamically adjusts its locations to provide stable and secure service to Bob. To this end, we denote the UAV's horizontal location in time slot n as $\mathbf{q}_n = [x_n, y_n]^T$ with a constant flight altitude H, which depends on the territorial building's height. In practice, the UAV is possibly influenced by environmental uncertainties, such as wind and weather impacts. To address these variations against secure communication design, in this section, we first introduce the UAV-enabled secure communication model, followed by presenting the trajectory control model.

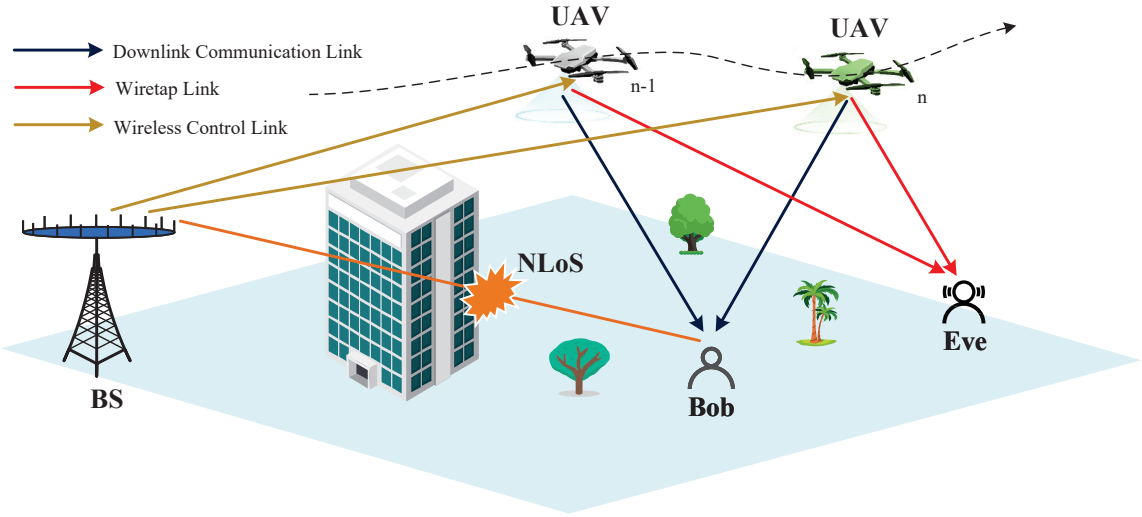

Figure 1. The considered UAV-assisted secure relay network.

2.1. Secure Communication Model

We consider that Bob and Eve are both on the ground with fixed locations, denoted by $\mathbf{q}_b = [x_b, y_b]^T$ and $\mathbf{q}_e = [x_e, y_e]^T$, respectively. For simplicity, we assume that the BS is located at $\mathbf{b}_0 = [0, 0]^T$. According to [36–38], we consider that the channels from UAV to Bob and Eve are both dominated by LoS links and the Doppler effect induced by UAV mobility can be well compensated. Consequently, the channel gain from the BS to UAV, the UAV to Bob and Eve can be respectively expressed as

$$h_{au,n} = \rho_0 d_{au,n}^{-2} = \frac{\rho_0}{H^2 + ||\mathbf{q}_n - \mathbf{b}_0||^2}, \quad n = 1, \cdots, N, \tag{1}$$

$$h_{ub,n} = \rho_0 d_{ub,n}^{-2} = \frac{\rho_0}{H^2 + ||\mathbf{q}_n - \mathbf{q}_b||^2}, \quad n = 1, \cdots, N, \tag{2}$$

$$h_{ue,n} = \rho_0 d_{ue,n}^{-2} = \frac{\rho_0}{H^2 + ||\mathbf{q}_n - \mathbf{q}_e||^2}, \quad n = 1, \cdots, N, \tag{3}$$

where $d_{au,n}$, $d_{ub,n}$, and $d_{ue,n}$ are the corresponding distances in time slot n. The term ρ_0 represents the channel gain at a unit reference distance. Denote $p_{0,n}$ and $p_{u,n}$ as the transmit powers associated with the BS and UAV in time slot n, respectively. Then, the corresponding achieved rates from the BS to UAV, the UAV to Bob and Eve can be respectively given by

$$R_{au,n} = \log_2(1 + \frac{p_{0,n}\rho_0/\sigma_0^2}{H^2 + ||\mathbf{q}_n - \mathbf{b}_0||^2}), \quad n = 1, \cdots, N, \tag{4}$$

 doi:10.20944/preprints202502.1810.v1

$$R_{ub,n} = \log_2(1 + \frac{p_{u,n}\rho_0/\sigma_0^2}{H^2 + ||\mathbf{q}_n - \mathbf{q}_b||^2}), \quad n = 1, \cdots, N, \tag{5}$$

$$R_{ue,n} = \log_2(1 + \frac{p_{u,n}\rho_0/\sigma_0^2}{H^2 + ||\mathbf{q}_n - \mathbf{q}_e||^2}), \quad n = 1, \cdots, N, \tag{6}$$

with σ_0^2 being the noise variance.

2.2. Trajectory Control Model

Once the optimal trajectory of the UAV is designed, the BS derives the corresponding control strategies, taking into account both the reference trajectory and the UAV's real-time state, and subsequently sends the commands to the UAV for path tracking. In this work, we assume that the uplink feedforward channel and the downlink feedback channel between the BS and the UAV are both ideal, as our focus is solely on the design of control strategies. This implies that the UAV can perfectly receive the control input, while the BS can accurately estimate the UAV's state. Specifically, we model the BS and the UAV as a liner control system, with the discrete-time system equations at time instant n formulated as [39–41]

$$\mathbf{q}_{n+1} = \mathbf{A}\mathbf{q}_n + \mathbf{B}\mathbf{v}_n, \tag{7}$$

$$\mathbf{y}_n = \mathbf{C}\mathbf{q}_n, \tag{8}$$

where $\mathbf{v}_n = \left[v_{x,n}, v_{y,n}\right]^{\mathrm{T}} \in \mathbb{R}^2$ denotes the control input, i.e, the UAV's velocity over the time interval $(n\triangle t, (n+1)\triangle t]$, $\mathbf{y}_n \in \mathbb{R}^2$ represents the UAV's state estimation result at the BS, $\mathbf{A}$, $\mathbf{B}$, and $\mathbf{C}$ are fixed state evolution matrix, input matrix, and deterministic matrix, respectively, defined as

$$\mathbf{A} = \mathbf{I}_{2\times 2}, \mathbf{B} = \begin{bmatrix} \triangle t & 0 \\ 0 & \triangle t \end{bmatrix} \in \mathbb{R}^{2\times 2}, \mathbf{C} = \mathbf{I}_{2\times 2}. \tag{9}$$

Furthermore, in light of the UAV's mechanical constraints, a new state-space model is introduced, where the increment in the UAV's velocity, defined as $\triangle\mathbf{v}_n = \mathbf{v}_n - \mathbf{v}_{n-1}$, is chosen as the control input. Simultaneously, the state-space variable $\mathbf{q}_n$ and the previous control input $\mathbf{v}_{n-1}$ are combined to form the new state $\hat{\mathbf{q}}_{n+1}$. Consequently, the discrete-time system equations are redefined as

$$\hat{\mathbf{q}}_{n+1} = \hat{\mathbf{A}}\hat{\mathbf{q}}_n + \hat{\mathbf{B}}\triangle\mathbf{v}_n, \tag{10}$$

$$\hat{\mathbf{y}}_n = \hat{\mathbf{C}}\hat{\mathbf{q}}_n, \tag{11}$$

where

$$\begin{cases} \hat{\mathbf{q}}_n = \begin{bmatrix} \mathbf{q}_n \\ \mathbf{v}_{n-1} \end{bmatrix} \in \mathbb{R}^4 \\ \hat{\mathbf{A}} = \begin{bmatrix} \mathbf{A} & \mathbf{B} \\ \mathbf{0}_{2\times 2} & \mathbf{I}_{2\times 2} \end{bmatrix} \in \mathbb{R}^{4\times 4}, \hat{\mathbf{B}} = \begin{bmatrix} \mathbf{B} \\ \mathbf{I}_{2\times 2} \end{bmatrix} \in \mathbb{R}^{4\times 2}, \\ \hat{\mathbf{C}} = \begin{bmatrix} \mathbf{C} & \mathbf{0}_{2\times 2} \end{bmatrix} \in \mathbb{R}^{2\times 4}, \hat{\mathbf{y}}_n = \mathbf{y}_n. \end{cases} \tag{12}$$

3. UAV Power Allocation and Trajectory Design

To counteract malicious eavesdropping, in this section, we focus on the joint optimization of UAV power allocation and trajectory design to ensure secure communication in UAV-assisted relay networks.

3.1. Problem Formulation

The secrecy rate $\tilde{R}_n$ in time slot n is defined as the difference between the achievable rate at Bob and Eve, i.e., $\tilde{R}_n = R_{ub,n} - R_{ue,n}$. The goal is to maximize the cumulative secrecy rate over the entire communication duration T by jointly taking into account the UAV transmit power $p_{u,n}$ and UAV

 doi:10.20944/preprints202502.1810.v1

trajectory $\mathbf{q}_n$. We further denote $\mathcal{P}_u = \{p_{u,n}, n = 1 \cdots N\}$ and $\mathcal{Q} = \{\mathbf{q}_n, n = 1 \cdots N\}$ as the variable sets that collect the UAV transmit power, and trajectory variables across all time slots. Consequently, the secrecy rate maximization problem can be formulated as:

$$\max_{\{\mathcal{P}_u, \mathcal{Q}\}} \sum_{n=1}^{N} \tilde{R}_n \tag{13a}$$

$$\text{s.t. } R_{ub,n} \leq R_{au,n}, \quad \forall n, \tag{13b}$$

$$||\mathbf{q}_{n+1} - \mathbf{q}_n|| \leq V_{\max}\Delta t, \quad \forall n, \tag{13c}$$

$$\sum_{n=1}^{N} p_{u,n} \leq P_{\max,u}, \quad p_{u,n} \geq 0, \quad \forall n, \tag{13d}$$

$$\mathbf{q}_1 = \mathbf{q}_I, \mathbf{q}_N = \mathbf{q}_F, \tag{13e}$$

where $V_{\max}$ is the maximum velocity of the UAV and $P_{\max,u}$ denotes the maximum transmit power budget corresponding to the UAV, respectively. $\mathbf{q}_I$ and $\mathbf{q}_F$ are the preset initial and final point. Constraint (13b) ensures that the achievable rate at Bob must not exceed the received rate at the UAV, while constraint (13c) denotes the UAV maximum travel distance within a single time slot. Moreover, constraint (13e) requires that the UAV return to its original at the end. Nevertheless, it is worth mentioning that problem (13) is non-convex, and consequently, it is challenging to deal with (13) by utilizing the traditional convex optimization methods. As a compromise, we propose a computationally efficient algorithm to obtain a locally optimal solution in what follows.

3.2. Efficient Solutions

In this subsection, we propose an AO-based algorithm to transform the original problem into a series of sub-problems and solve them iteratively to obtain an efficient solution. In particular, problem (13) can be decomposed into two subproblems, i.e., sub-problem 1: optimizing transmit powers with a fixed trajectory and sub-problem 2: optimizing the trajectory with other variables fixed. To begin with, we solve subproblem 1, which can be particularized as

$$\max_{\{\mathcal{P}_u\}} \sum_{n=1}^{N} \log_2(1 + p_{u,n}\gamma_{ub,n}) - \log_2(1 + p_{u,n}\gamma_{ue,n}) \tag{14a}$$

$$\text{s.t. } \log_2(1 + p_{u,n}\gamma_{ub,n}) \leq R_{au,n}, \quad \forall n, \tag{14b}$$

$$\sum_{n=1}^{N} p_{u,n} \leq P_{\max,u}, \quad p_{u,n} \geq 0, \quad \forall n, \tag{14c}$$

where $\gamma_{ub,n} = h_{ub,n}/\sigma_0^2$ and $\gamma_{ue,n} = h_{ue,n}/\sigma_0^2$. Although problem (14) is still non-convex, it can be iteratively solved by adopting the SCA technique. Specifically, the non-convex term in the objective function is $-\log_2(1 + p_{u,n}\gamma_{ue,n})$. In the k-th iteration, we approximate this term by performing a first-order Taylor expansion around the current power allocation $p_{u,n}^{(k)}$, i.e.,

$$\log_2(1 + p_{u,n}\gamma_{ue,n}) \approx \log_2\left(1 + p_{u,n}^{(k)}\gamma_{ue,n}\right) + \frac{\gamma_{ue,n}}{\ln 2\left(1 + p_{u,n}^{(k)}\gamma_{ue,n}\right)}\left(p_{u,n} - p_{u,n}^{(k)}\right) \triangleq \hat{R}_{ue,n}. \tag{15}$$

Substitute (15) into the objective function, we arrive at the following convex approximation

$$\tilde{R}_n \approx \sum_{n=1}^{N} \left[\log_2(1 + p_{u,n}\gamma_{ub,n}) - \hat{R}_{ue,n}.\right] \tag{16}$$

 doi:10.20944/preprints202502.1810.v1

Hence, in the k-th iteration, the following convex optimization problem is solved:

$$\begin{aligned} &\max_{\{\mathcal{P}_u\}} \sum_{n=1}^{N} \tilde{R}_n \\ &\text{s.t. } p_{u,n} \le (2^{R_{au,n}} - 1)/\gamma_{ub,n}, \quad \forall n, \\ &\quad \sum_{n=1}^{N} p_{u,n} \le P_{\max,u}, \quad p_{u,n} \ge 0, \quad \forall n. \end{aligned} \tag{17}$$

Problem (18) now is convex and thus can be efficiently addressed via standard solvers, e.g., CVX [42]. Subsequently, we optimize the UAV trajectory given the power variable $\mathcal{P}_u$, which is given by

$$\max_{\mathcal{Q}} \sum_{n=1}^{N} \log_2(1 + \frac{\beta_{u,n}}{H^2 + ||\mathbf{q}_n - \mathbf{q}_b||^2}) - \log_2(1 + \frac{\beta_{u,n}}{H^2 + ||\mathbf{q}_n - \mathbf{q}_e||^2}) \tag{18a}$$

$$\text{s.t. } \log_2(1 + \frac{\beta_{u,n}}{H^2 + ||\mathbf{q}_n - \mathbf{q}_b||^2}) \le \log_2(1 + \frac{\beta_{0,n}}{H^2 + ||\mathbf{q}_n - \mathbf{b}_0||^2}) \quad \forall n, \tag{18b}$$

$$||\mathbf{q}_{n+1} - \mathbf{q}_n|| \le V_{\max}\Delta t, \quad \forall n, \tag{18c}$$

$$\mathbf{q}_1 = \mathbf{q}_I, \mathbf{q}_N = \mathbf{q}_F, \tag{18d}$$

with $\beta_{u,n} = p_{u,n}\rho_0/\sigma_0^2$ and $\beta_{0,n} = p_{0,n}\rho_0/\sigma_0^2$. We first note that $R_{ub,n}$ has a convex lower-bound at the given point $\mathbf{q}_n^r$ by invoking the SCA method, such that we arrive

$$R_{ub,n}^{lb} \ge \log_2\left(1 + \frac{\beta_{u,n}}{H^2 + \|\mathbf{q}_n^r - \mathbf{q}_b\|^2}\right) - \frac{\beta_{u,n}}{\ln 2}\left(\frac{1}{1 + \frac{\beta_{u,n}}{(H^2 + \|\mathbf{q}_n^r - \mathbf{q}_b\|^2)}}\right) \times \frac{\|\mathbf{q}_n - \mathbf{q}_b\|^2 - \|\mathbf{q}_n^r - \mathbf{q}_b\|^2}{\left(H^2 + \|\mathbf{q}_n^r - \mathbf{q}_b\|^2\right)^2}. \tag{19}$$

Moreover, introducing an auxiliary variable $\theta_n = ||\mathbf{q}_n - \mathbf{q}_e||^2$, we can transform the objective function into a convex form with an additional constraint

$$\theta_n \le \|\mathbf{q}_n^r - \mathbf{q}_e\|^2 + 2(\mathbf{q}_n^r - \mathbf{q}_e)^{\mathrm{T}}(\mathbf{q}_n - \mathbf{q}_n^r). \tag{20}$$

Similarly, one can employ SCA technique to convert constraint (18b) into

$$\beta_{u,n}\left(H^2 + \|\mathbf{q}_n - \mathbf{b}_0\|^2\right) \le \beta_{0,n}\left(\|\mathbf{q}_n^r - \mathbf{q}_b\|^2 + 2(\mathbf{q}_n^r - \mathbf{q}_b)^T(\mathbf{q}_n - \mathbf{q}_n^r)\right). \tag{21}$$

As a result, problem (18) can be approximated as

$$\begin{aligned} &\max_{\mathcal{Q},\theta_n} \sum_{n=1}^{N} R_{ub,n}^{lb} - \log_2(1 + \beta_{u,n}/(H^2 + \theta_n)) \\ &\quad \text{s.t. } (18c), (18d), (20), (21), \end{aligned} \tag{22}$$

which is a convex problem and can be solved by CVX[43]. In a nutshell, the original problem can be solved by iteratively dealing with problems (18) and (22). Since there exists a finite upper bound due to the power constraint, the proposed algorithm can be guaranteed to converge.

4. MPC-Based Trajectory Tracking

In this section, we employ a MPC-based approach to achieve precise trajectory tracking. The primary objective of MPC is to compute a sequence of control inputs within the prediction horizon, denoted as N_1, thereby minimizing the deviation between the reference path optimized in Section 3

 doi:10.20944/preprints202502.1810.v1

and the trajectory predicted by the MPC framework. Accordingly, the control cost function at time instant n is formulated as [44]

$$J_n = \sum_{i=0}^{N_1-1} \mathbf{e}_{n+i|n}^{\mathrm{T}} \mathbf{R}_1 \mathbf{e}_{n+i|n} + \triangle \mathbf{v}_{n+i|n}^{\mathrm{T}} \mathbf{R}_2 \triangle \mathbf{v}_{n+i|n} + \mathbf{e}_{n+N}^{\mathrm{T}} \mathbf{R}_3 \mathbf{e}_{n+N} \tag{23}$$

where $\mathbf{e}_n = \hat{\mathbf{q}}_n - \hat{\mathbf{q}}_{n,\mathrm{ref}}$ represents the error between the true state and the reference optimal state, $\mathbf{e}_{n+i|n}$ indicates the predicted state deviation at time instant $n+i$, given $\mathbf{e}_{n|n} = \mathbf{e}_n$, $\triangle \mathbf{v}_{n+i|n}$ denotes the control input at time $n+i$, predicted at time n, while $\mathbf{R}_1 \in \mathbb{R}^{4\times4}$ and $\mathbf{R}_2 \in \mathbb{R}^{2\times2}$ are positive definite weighting matrices for the states and inputs, respectively. In (23), the first term corresponds to the state cost, which penalizes deviations from the reference state $\hat{\mathbf{q}}_{n,\mathrm{ref}}$. The second term represents the input cost, penalizing deviations from the steady-state input. Finally, the third term corresponds to the terminal cost, which compensates for the control cost and approximates the result for $N_1 = \infty$, thereby enhancing control performance, where $\mathbf{R}_3 \in \mathbb{R}^{4\times4}$ is the solution to the discrete Riccati function [45], given by

$$\mathbf{R}_3 = \mathbf{R}_1 + \hat{\mathbf{A}}^{\mathrm{T}} \mathbf{R}_3 \hat{\mathbf{A}} - \hat{\mathbf{A}}^{\mathrm{T}} \mathbf{R}_3 \hat{\mathbf{B}} \left(\mathbf{R}_2 + \hat{\mathbf{B}}^{\mathrm{T}} \mathbf{R}_3 \hat{\mathbf{B}} \right)^{-1} \hat{\mathbf{B}}^{\mathrm{T}} \mathbf{R}_3 \hat{\mathbf{A}}. \tag{24}$$

Given that perfect knowledge of the control state $\hat{\mathbf{q}}_n$ and control input $\triangle \mathbf{v}_n$ is available on the UAV and BS sides, the MPC-based trajectory tracking optimization problem is formulated as

$$\min_{\{\triangle \mathbf{v}_{n+i|n}\}_{i=0}^{N_1-1}} \quad J_n \tag{25a}$$

$$\text{s.t.} \quad \triangle \mathbf{v}_{n+i|n} \in \boldsymbol{v}, i = 0, \ldots, N_1 - 1, \tag{25b}$$

$$(10), (11), \tag{25c}$$

where (25b) denotes the control input constraint, with v representing the velocity increment limit of the UAV. Notably, while the control inputs for the entire prediction horizon can be obtained by solving problem (25), only the control input corresponding to the current sampling interval, i.e., $\mathbf{v}_n = \mathbf{v}_{n-1} + \triangle \mathbf{v}_n^{\star}$, is applied and transmitted to the UAV. At each subsequent time step, this process is repeated with updated information and a rolling prediction horizon.

To address the formulated problem, we begin by expressing J_n in a quadratic form. Using the control system equations (10) and (11), the predicted control states over the prediction horizon are computed as

$$\begin{aligned}
\hat{\mathbf{q}}_{n|n} &= \hat{\mathbf{q}}_n, \\
\hat{\mathbf{q}}_{n+1|n} &= \hat{\mathbf{A}} \hat{\mathbf{q}}_n + \hat{\mathbf{B}} \triangle \mathbf{v}_{n|n}, \\
\hat{\mathbf{q}}_{n+2|n} &= \hat{\mathbf{A}} \hat{\mathbf{q}}_{n+1|n} + \hat{\mathbf{B}} \triangle \mathbf{v}_{n+1|n} \\
&= \hat{\mathbf{A}}^2 \hat{\mathbf{q}}_n + \hat{\mathbf{A}} \hat{\mathbf{B}} \triangle \mathbf{v}_{n|n} + \hat{\mathbf{B}} \triangle \mathbf{v}_{n+1|n}, \\
&\vdots \\
\hat{\mathbf{q}}_{n+N_1|n} &= \hat{\mathbf{A}}^{N_1} \hat{\mathbf{q}}_n + \hat{\mathbf{A}}^{N_1-1} \hat{\mathbf{B}} \triangle \mathbf{v}_{n|n} + \ldots + \hat{\mathbf{B}} \triangle \mathbf{v}_{n+N_1-1|n},
\end{aligned} \tag{26}$$

which can be expressed as the matrix form, i.e,

$$\mathbf{Q}_n = \mathbf{M} \hat{\mathbf{q}}_n + \mathbf{F} \triangle \mathbf{V}_n, \tag{27}$$

 doi:10.20944/preprints202502.1810.v1

where $\mathbf{Q}_n$ and $\triangle\mathbf{V}_n$ represent the new control state and input matrices, respectively, which are defined as

$$\mathbf{Q}_n = \begin{bmatrix} \hat{\mathbf{q}}_{n|n} \\ \hat{\mathbf{q}}_{n+1|n} \\ \vdots \\ \hat{\mathbf{q}}_{n+N_1|n} \end{bmatrix} \in \mathbb{R}^{4N_1+4}, \triangle\mathbf{V}_n = \begin{bmatrix} \triangle\mathbf{v}_{n|n} \\ \triangle\mathbf{v}_{n+1|n} \\ \vdots \\ \triangle\mathbf{v}_{n+N_1-1|n} \end{bmatrix} \in \mathbb{R}^{2N_1}, \tag{28}$$

with

$$\mathbf{M} = \begin{bmatrix} \mathbf{I}_{4\times4} \\ \hat{\mathbf{A}} \\ \vdots \\ \hat{\mathbf{A}}^{N_1} \end{bmatrix} \in \mathbb{R}^{(4N_1+4)\times4}, \mathbf{F} = \begin{bmatrix} \mathbf{0} & \mathbf{0} & \cdots & \mathbf{0} \\ \hat{\mathbf{B}} & \mathbf{0} & \cdots & \mathbf{0} \\ \hat{\mathbf{A}}\hat{\mathbf{B}} & \hat{\mathbf{B}} & \cdots & \mathbf{0} \\ \vdots & \vdots & \ddots & \vdots \\ \hat{\mathbf{A}}^{N_1-1}\hat{\mathbf{B}} & \hat{\mathbf{A}}^{N_1-2}\hat{\mathbf{B}} & \cdots & \hat{\mathbf{B}} \end{bmatrix} \in \mathbb{R}^{(4N_1+4)\times2N_1}. \tag{29}$$

Let us denote the reference state matrix as

$$\mathbf{Q}_{n,\text{ref}} = \begin{bmatrix} \hat{\mathbf{q}}_{k,\text{ref}} \\ \hat{\mathbf{q}}_{n+1,\text{ref}} \\ \vdots \\ \hat{\mathbf{q}}_{n+N_1,\text{ref}} \end{bmatrix} \in \mathbb{R}^{4N_1+4}, \tag{30}$$

which includes the reference position and velocity of the UAV over the prediction horizon. Consequently, the control cost is equivalently reformulated as

$$J_n = (\mathbf{Q}_n - \mathbf{Q}_{n,\text{ref}})^{\mathrm{T}}\bar{\mathbf{R}}_1(\mathbf{Q}_n - \mathbf{Q}_{n,\text{ref}}) + \triangle\mathbf{V}_n^{\mathrm{T}}\bar{\mathbf{R}}_2\triangle\mathbf{V}_n, \tag{31}$$

where $\bar{\mathbf{R}}_1 = \text{diag}(\mathbf{R}_1, \ldots, \mathbf{R}_1, \mathbf{R}_3)$ and $\bar{\mathbf{R}}_2 = \text{diag}(\mathbf{R}_2, \ldots, \mathbf{R}_2)$. Substituting (27) into (31) yields the reformulated control cost function

$$J_n = \triangle\mathbf{V}_n^{\mathrm{T}}\mathbf{H}\triangle\mathbf{V}_n + \mathbf{E}\triangle\mathbf{V}_n + G, \tag{32}$$

where

$$\mathbf{H} = \mathbf{F}^{\mathrm{T}}\bar{\mathbf{R}}_1\mathbf{F} + \bar{\mathbf{R}}_2, \tag{33}$$

$$\mathbf{E} = 2\left(\hat{\mathbf{q}}_n^{\mathrm{T}}\mathbf{M}^{\mathrm{T}} - \mathbf{Q}_{n,\text{ref}}^{\mathrm{T}}\right)\bar{\mathbf{R}}_1\mathbf{F}, \tag{34}$$

$$G = \hat{\mathbf{q}}_n^{\mathrm{T}}\mathbf{M}^{\mathrm{T}}\bar{\mathbf{R}}_1\mathbf{M}\hat{\mathbf{q}}_n - 2\hat{\mathbf{q}}_n^{\mathrm{T}}\mathbf{M}^{\mathrm{T}}\bar{\mathbf{R}}_1\mathbf{Q}_{n,\text{ref}} + \mathbf{Q}_{n,\text{ref}}^{\mathrm{T}}\bar{\mathbf{R}}_1\mathbf{Q}_{n,\text{ref}}. \tag{35}$$

Therefore, problem (25) is equivalently transformed into

$$\min_{\triangle\mathbf{V}_n} \quad J_n \tag{36a}$$

$$\text{s.t.} \quad \triangle\mathbf{V}_n \in \boldsymbol{V}, \tag{36b}$$

where $\boldsymbol{V}$ constrains the control input matrix $\triangle\mathbf{V}_n$. Since the objective function J_n is quadratic with positive definite weighting matrix $\mathbf{H}$, problem (36) can be efficiently solved as a convex QP problem by employing standard techniques [43], [42]. At every time slot, the MPC-based optimization problem is solved and the optimal control input is calculated as $\triangle\mathbf{v}_n^\star = (\triangle\mathbf{V}_n^\star)_1$, where$(\triangle\mathbf{V}_n^\star)_1$ corresponds to the first two elements of $\triangle\mathbf{V}_n^\star \in \mathbb{R}^{2N_1}$.

5. Simulation Results

In this section, we present the simulation results to verify the effectiveness of our proposed algorithm. Unless otherwise specified, the system parameters are set as follows: the maximum UAV

Preprints.org (www.preprints.org) | NOT PEER-REVIEWED | Posted: 24 February 2025 doi:10.20944/preprints202502.1810.v1

speed is $V_{\max} = 30$ m/s, the channel gain at a unit reference distance is $\rho_0 = -60$ dB and the received noise at the receivers is set to $\sigma_0^2 = -110$ dBm. The locations corresponding to the BS, Bob, and Eve are set to $\mathbf{b}_0 = [100, 300]^T$ m, $\mathbf{q}_b = [200, 0]^T$ m, and $\mathbf{q}_e = [400, 300]^T$ m, respectively. Moreover, we set the initial point and the final point to $\mathbf{q}_I = [500, 0]^T$ m and $\mathbf{q}_F = [100, 400]^T$ m, respectively. As for the control part, the weighting matrices for the states and inputs, $\mathbf{R}_1$ and $\mathbf{R}_2$, are both identity matrices.

Figure 2 illustrates the UAV's trajectory under varying total durations, demonstrating how the UAV dynamically adjusts its path to optimize secure communication. As the total mission duration increases, the UAV's trajectory becomes closer to Bob and the BS. This is because a longer flight time enables the UAV to better fly away from Eve. The trajectory for the $T = 60$ s demonstrates a steeper descent toward the final position, reflecting a more direct path to the goal. In contrast, the trajectory for the longer duration $T = 100$ s is more gradual, indicating that the UAV takes a longer path to the final position. This behavior is expected as the UAV has more time to adjust its trajectory, potentially avoiding eavesdropping. Moreover, the UAV tends to hover closer to Bob during critical communication periods for enhancing the system throughput.

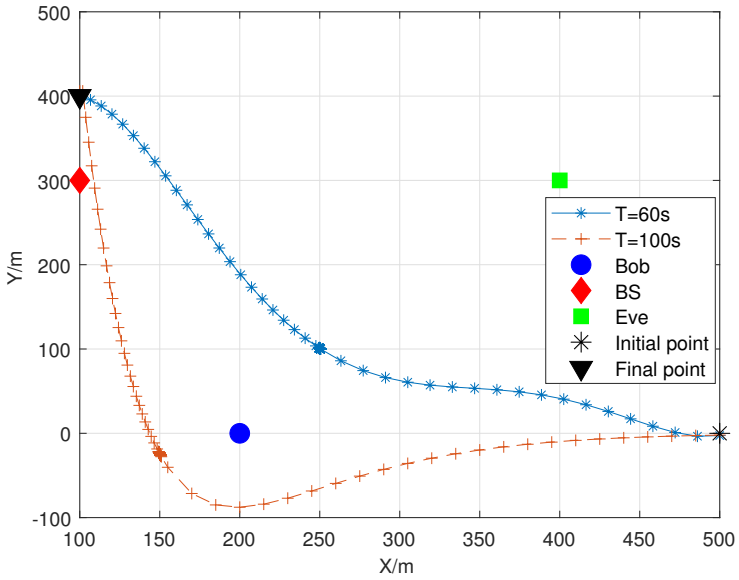

Figure 2. The optimized UAV trajectory under different total durations.

Figure 3 depicts the average secrecy rate as a function of time duration for different transmit powers compared to the benchmark scheme straight flight approach, in which the UAV directly flies from the initial point to the destination. It is evident that for both proposed and straight flight trajectories, increasing the transmit power from 5 W to 10 W results in a higher average secrecy rate, highlighting the trade-off between power and security. Furthermore, the proposed design, which adapts the UAV's trajectory based on the available time, outperforms the straight-flight approach in all cases, suggesting that adjusting the UAV's flight path can significantly enhance communication security, especially when combined with higher transmit power. Additionally, the average secrecy rate tends to stabilize over longer durations. The reason is that the UAV, with long flight durations, is capable of flying to hover over Bob, providing considerable communication service.

 doi:10.20944/preprints202502.1810.v1

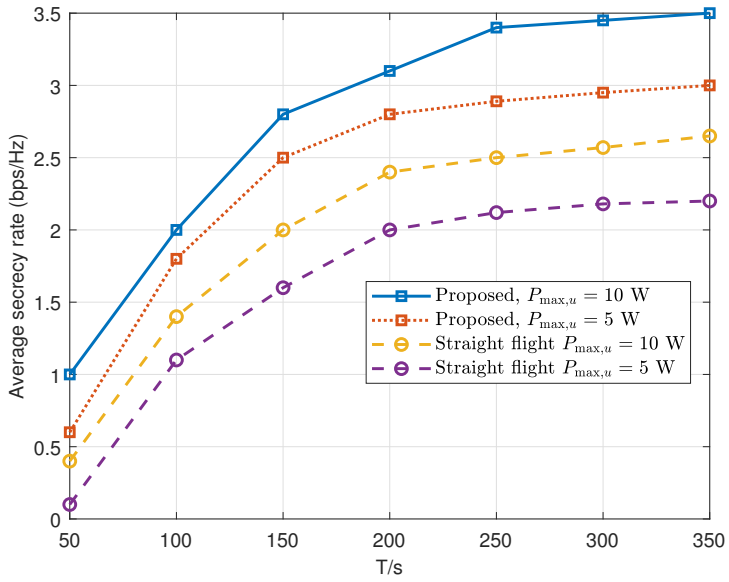

Figure 3. Average secrecy rate versus time duration with different transmit powers.

Figure 4 illustrates the UAV's trajectory tracking performance using MPC. At the start, a noticeable deviation from the reference path occurs as the UAV adjusts its velocity and position to align with the desired trajectory. Similarly, some tracking errors appear at the hovering position, likely due to the difficulty in maintaining precise stabilization. However, as the UAV progresses, the tracking accuracy improves significantly, closely following the reference path. This demonstrates the effectiveness of the MPC controller in continuously refining the UAV's motion, enabling smooth and accurate trajectory tracking despite initial deviations. Figure 5 shows the cumulative distribution function (CDF) of the mean squared error (MSE) between the UAV's actual trajectory and the reference trajectory under different prediction horizons. The MSE quantifies the tracking error, with lower values indicating better adherence to the reference path. As expected, the CDF curve shifts to the right as the prediction horizon decreases, with the $N_1 = 20$ case achieving the best tracking performance, showing a higher proportion of lower MSE values. This demonstrates that a larger prediction horizon allows the MPC controller to plan further ahead, leading to more accurate trajectory tracking. As the prediction horizon decreases, the controller has less foresight, which results in larger tracking errors. This highlights the importance of a sufficiently large prediction horizon for optimal trajectory tracking in dynamic environments.

 doi:10.20944/preprints202502.1810.v1

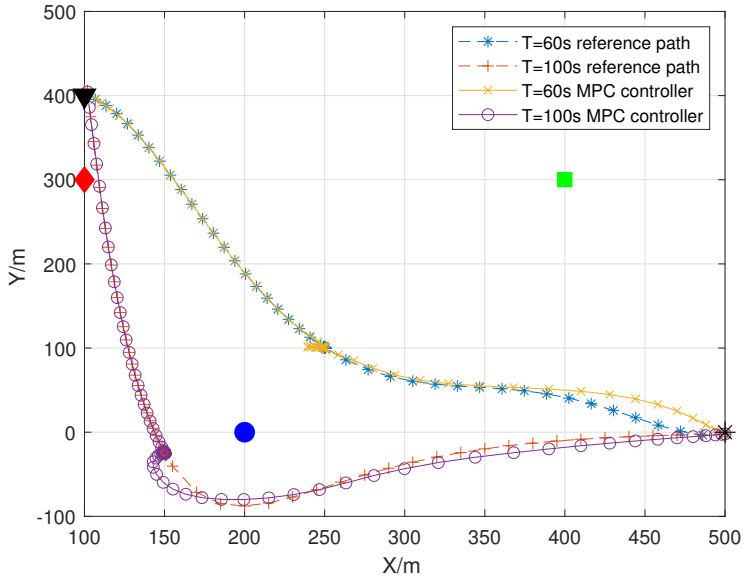

Figure 4. MPC-based tracking path under different total durations.

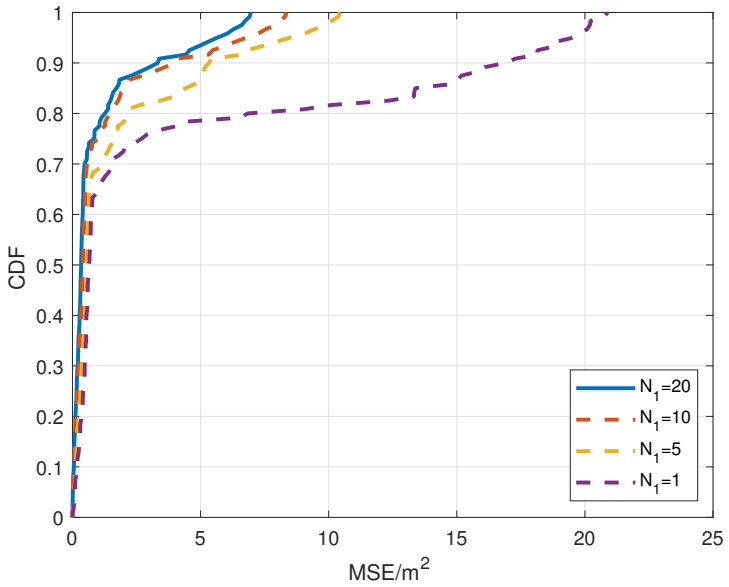

Figure 5. CDF of MSE perfoemance with different prediction horizons with $T = 60$ s.

6. Conslusions

In this paper, we have presented a novel framework for secure communications in UAV-assisted relay networks. Our approach jointly optimized the UAV's transmit power and trajectory, addressing the security vulnerabilities posed by the reliance on LoS channels. By employing a MPC-based approach, we have demonstrated how the UAV's trajectory can be adaptively controlled in real-time, improving the resilience of the system against dynamic environmental conditions and potential eavesdropping threats. We first formulated a non-convex secrecy rate maximization problem and proposed an efficient solution using SCA techniques. The MPC-based path tracking ensured that the UAV could follow the optimized trajectory efficiently, even under practical constraints and disturbances. Simulation results show that the proposed joint optimization framework significantly enhances communication security, providing robust performance under dynamic conditions.

 doi:10.20944/preprints202502.1810.v1

Author Contributions: Conceptualization, S.L.; methodology, S.L. and L.Z.; resources, B.T. and Y.L.; writing-original draft preparation, S.L., L.Z. and S.C.; writing-review and editing, S.C. and H.X.; Supervision, H.X.; funding acquisition, H.X.. All authors have read and agreed to the published version of the manuscript.

Funding: Not applicable.

Institutional Review Board Statement: Not applicable.

Informed Consent Statement: Not applicable.

Data Availability Statement: Not applicable.

Acknowledgments: Not applicable.

Conflicts of Interest: The authors declare no conflict of interest.

References

1. Motlagh, N.H.; Bagaa, M.; Taleb, T. UAV-Based IoT Platform: A Crowd Surveillance Use Case. *IEEE Commun. Mag.* **2017**, *55*, 128–134. https://doi.org/10.1109/MCOM.2017.1600587CM.
2. Wu, J.; Yuan, W.; Bai, L. On the Interplay Between Sensing and Communications for UAV Trajectory Design. *IEEE Internet of Things Journal* **2023**, *10*, 20383–20395. https://doi.org/10.1109/JIOT.2023.3287991.
3. Liu, Y.; Shi, Y.; Zhang, X.; Wu, J.; Yang, S. Reinforcement Learning-Based Car-Following Control for Autonomous Vehicles with OTFS. In Proceedings of the 2024 IEEE Wireless Communications and Networking Conference (WCNC), 2024, pp. 1–6. https://doi.org/10.1109/WCNC57260.2024.10570722.
4. Lu, S.; Liu, F.; Li, Y.; Zhang, K.; Huang, H.; Zou, J.; Li, X.; Dong, Y.; Dong, F.; Zhu, J.; et al. Integrated Sensing and Communications: Recent Advances and Ten Open Challenges. *IEEE Internet of Things Journal* **2024**, *11*, 19094–19120. https://doi.org/10.1109/JIOT.2024.3361173.
5. Li, B.; Yuan, W.; Liu, F.; Wu, N.; Jin, S. OTFS-Based ISAC: How Delay Doppler Channel Estimation Assists Environment Sensing? *IEEE Wireless Communications Letters* **2024**, *13*, 3563–3567. https://doi.org/10.1109/LWC.2024.3478744.
6. De Freitas, E.P.; Heimfarth, T.; Netto, I.F.; Lino, C.E.; Pereira, C.E.; Ferreira, A.M.; Wagner, F.R.; Larsson, T. UAV relay network to support WSN connectivity. In Proceedings of the international congress on ultra modern telecommunications and control systems. IEEE, 2010, pp. 309–314.
7. Wu, J.; Yuan, W.; Wei, Z.; Zhang, K.; Liu, F.; Wing Kwan Ng, D. Low-Complexity Minimum BER Precoder Design for ISAC Systems: A Delay-Doppler Perspective. *IEEE Transactions on Wireless Communications* **2025**, *24*, 1526–1540. https://doi.org/10.1109/TWC.2024.3509973.
8. Zhan, P.; Yu, K.; Swindlehurst, A.L. Wireless relay communications with unmanned aerial vehicles: Performance and optimization. *IEEE Transactions on Aerospace and Electronic Systems* **2011**, *47*, 2068–2085.
9. Li, B.; Zhao, S.; Miao, R.; Zhang, R. A survey on unmanned aerial vehicle relaying networks. *IET communications* **2021**, *15*, 1262–1272.
10. Choi, D.H.; Kim, S.H.; Sung, D.K. Energy-efficient maneuvering and communication of a single UAV-based relay. *IEEE Transactions on Aerospace and Electronic Systems* **2014**, *50*, 2320–2327. https://doi.org/10.1109/TAES.2013.130074.
11. Zeng, Y.; Zhang, R.; Lim, T.J. Throughput Maximization for UAV-Enabled Mobile Relaying Systems. *IEEE Transactions on Communications* **2016**, *64*, 4983–4996. https://doi.org/10.1109/TCOMM.2016.2611512.
12. Zhang, S.; Zhang, H.; He, Q.; Bian, K.; Song, L. Joint trajectory and power optimization for UAV relay networks. *IEEE Communications Letters* **2017**, *22*, 161–164.
13. Sun, G.; Li, N.; Tao, X.; Wu, H. Power allocation in UAV-enabled relaying systems for secure communications. *IEEE Access* **2019**, *7*, 119009–119017.
14. Zhang, X.; Huang, H.; Tan, L.; Yuan, W.; Liu, C. Enhanced Channel Estimation for OTFS-Assisted ISAC in Vehicular Networks: A Deep Learning Approach. In Proceedings of the 2023 21st International Symposium on Modeling and Optimization in Mobile, Ad Hoc, and Wireless Networks (WiOpt), 2023, pp. 703–707. https://doi.org/10.23919/WiOpt58741.2023.10349836.
15. Zhang, X.; Yuan, W.; Liu, C.; Wu, J.; Ng, D.W.K. Predictive Beamforming for Vehicles With Complex Behaviors in ISAC Systems: A Deep Learning Approach. *IEEE Journal of Selected Topics in Signal Processing* **2024**, *18*, 828–841. https://doi.org/10.1109/JSTSP.2024.3405856.

 doi:10.20944/preprints202502.1810.v1

16. Yuan, W.; Wei, Z.; Li, S.; Yuan, J.; Ng, D.W.K. Integrated Sensing and Communication-Assisted Orthogonal Time Frequency Space Transmission for Vehicular Networks. *IEEE Journal of Selected Topics in Signal Processing* **2021**, *15*, 1515–1528. https://doi.org/10.1109/JSTSP.2021.3117404.
17. Zhu, J.; Jin, H.; He, Y.; Fang, F.; Huang, W.; Zhang, Z. Joint Optimization of User Scheduling, Rate Allocation, and Beamforming for RSMA Finite Blocklength Transmission. *IEEE Internet of Things Journal* **2024**, *11*, 27904–27915. https://doi.org/10.1109/JIOT.2024.3420099.
18. Tan, L.; Yuan, W.; Zhang, X.; Zhang, K.; Li, Z.; Li, Y. DNN-Based Radar Target Detection With OTFS. *IEEE Transactions on Vehicular Technology* **2024**, *73*, 15786–15791. https://doi.org/10.1109/TVT.2024.3408059.
19. Wu, J.; Yuan, W.; Hanzo, L. When UAVs Meet ISAC: Real-Time Trajectory Design for Secure Communications. *IEEE Transactions on Vehicular Technology* **2023**, *72*, 16766–16771. https://doi.org/10.1109/TVT.2023.3290033.
20. He, D.; Chan, S.; Guizani, M. Communication security of unmanned aerial vehicles. *IEEE Wireless Communications* **2016**, *24*, 134–139.
21. Wu, J.; Yuan, W.; Bai, L. Multi-UAV Enabled Sensing: Cramér-Rao Bound Optimization. In Proceedings of the 2023 IEEE International Conference on Communications Workshops (ICC Workshops), 2023, pp. 925–930. https://doi.org/10.1109/ICCWorkshops57953.2023.10283770.
22. Rodday, N.M.; Schmidt, R.d.O.; Pras, A. Exploring security vulnerabilities of unmanned aerial vehicles. In Proceedings of the NOMS 2016-2016 IEEE/IFIP Network Operations and Management Symposium. IEEE, 2016, pp. 993–994.
23. Wang, Q.; Chen, Z.; Mei, W.; Fang, J. Improving Physical Layer Security Using UAV-Enabled Mobile Relaying. *IEEE Wireless Communications Letters* **2017**, *6*, 310–313. https://doi.org/10.1109/LWC.2017.2680449.
24. Wang, Q.; Chen, Z.; Li, H.; Li, S. Joint Power and Trajectory Design for Physical-Layer Secrecy in the UAV-Aided Mobile Relaying System. *IEEE Access* **2018**, *6*, 62849–62855. https://doi.org/10.1109/ACCESS.2018.2877210.
25. Zhang, G.; Wu, Q.; Cui, M.; Zhang, R. Securing UAV Communications via Trajectory Optimization. In Proceedings of the GLOBECOM 2017 - 2017 IEEE Global Communications Conference, 2017, pp. 1–6. https://doi.org/10.1109/GLOCOM.2017.8254971.
26. Ryan, A.; Zennaro, M.; Howell, A.; Sengupta, R.; Hedrick, J. An overview of emerging results in cooperative UAV control. In Proceedings of the 2004 43rd IEEE Conference on Decision and Control (CDC) (IEEE Cat. No.04CH37601), 2004, Vol. 1, pp. 602–607 Vol.1. https://doi.org/10.1109/CDC.2004.1428700.
27. Li, Z.; Yuan, W.; Li, B.; Wu, J.; You, C.; Meng, F. Reconfigurable-Intelligent-Surface-Aided OTFS: Transmission Scheme and Channel Estimation. *IEEE Internet of Things Journal* **2023**, *10*, 19518–19532. https://doi.org/10.1109/JIOT.2023.3270335.
28. Jin, H.; Wu, J.; Yuan, W.; Liu, F.; Yuanhao, C. Co-Design of Sensing, Communication, and Control for Low-Altitude Wireless Networks with Finite Blocklength Transmission. *Submitted to IEEE Transactions on Mobile Computing* **2025**.
29. Baek, H.; Lim, J. Design of future UAV-relay tactical data link for reliable UAV control and situational awareness. *IEEE Communications Magazine* **2018**, *56*, 144–150.
30. Zhang, X.; Yuan, W.; Liu, C.; Wu, J.; Li, Z. Deep Learning-Based Cramér-Rao Bound Optimization for Integrated Sensing and Communication in Vehicular Networks. In Proceedings of the 2023 IEEE 24th International Workshop on Signal Processing Advances in Wireless Communications (SPAWC), 2023, pp. 646–650. https://doi.org/10.1109/SPAWC53906.2023.10304366.
31. Zhang, X.; Liu, C.; Yuan, W.; Zhang, J.A.; Ng, D.W.K. Sparse Prior-Guided Deep Learning for OTFS Channel Estimation. *IEEE Transactions on Vehicular Technology* **2024**, *73*, 19913–19918. https://doi.org/10.1109/TVT.2024.3450012.
32. Yuan, W.; Yang, Z.; Chen, L.; Zhang, R.; Yao, Y.; Cui, Y.; Zhang, H.; Ng, D.W.K. Wireless Localization and Formation Control With Asynchronous Agents. *IEEE Journal on Selected Areas in Communications* **2024**, *42*, 2890–2904. https://doi.org/10.1109/JSAC.2024.3414616.
33. Sir Elkhatem, A.; Naci Engin, S. Robust LQR and LQR-PI control strategies based on adaptive weighting matrix selection for a UAV position and attitude tracking control. *Alexandria Engineering Journal* **Aug. 2022**, *61*, 6275–6292. https://doi.org/https://doi.org/10.1016/j.aej.2021.11.057.
34. Lu, S.; Liu, F.; Dong, F.; Xiong, Y.; Xu, J.; Liu, Y.F.; Jin, S. Random ISAC signals deserve dedicated precoding. *IEEE Transactions on Signal Processing* **2024**.
35. Chao, Z.; Ming, L.; Shaolei, Z.; Wenguang, Z. Collision-free UAV formation flight control based on nonlinear MPC. In Proceedings of the 2011 international conference on electronics, communications and control (ICECC). IEEE, 2011, pp. 1951–1956.

 doi:10.20944/preprints202502.1810.v1

36. Wu, J.; Yuan, W.; Cheng, Q.; Jin, H. Towards Dual-Functional LAWN: Control-Aware System Design for Aerodynamics-Aided UAV Formations. *Submitted to IEEE IEEE Journal on Selected Areas in Communications* **2025**.
37. Zhang, K.; Wu, J.; Dong, F.; Lu, S.; Li, X.; Yuan, W. Joint Design of Receiving Filters and Complementary set of Sequences for ISAC With Sidelobe Level Suppression. *IEEE Journal of Selected Areas in Sensors* **2024**, *1*, 211–223. https://doi.org/10.1109/JSAS.2024.3462687.
38. Wu, J.; Yuan, W.; Liu, F.; Cui, Y.; Meng, X.; Huang, H. UAV-Based Target Tracking: Integrating Sensing into Communication Signals. In Proceedings of the 2022 IEEE/CIC International Conference on Communications in China (ICCC Workshops), 2022, pp. 309–313. https://doi.org/10.1109/ICCCWorkshops55477.2022.9896671.
39. Amato, F.; Ariola, M. Finite-time control of discrete-time linear systems. *IEEE Transactions on Automatic Control* **2005**, *50*, 724–729. https://doi.org/10.1109/TAC.2005.847042.
40. Shi, Y.; Li, B.; Wei, X.; Huang, H. Experimental Implementation of an OTFS-Based ISAC System. In Proceedings of the 2024 IEEE/CIC International Conference on Communications in China (ICCC Workshops), 2024, pp. 587–592. https://doi.org/10.1109/ICCCWorkshops62562.2024.10693814.
41. Zhang, K.; Yuan, W.; Fan, P.; Wang, X. Dual-Functional Waveform Design With Local Sidelobe Suppression via OTFS Signaling. *IEEE Transactions on Vehicular Technology* **2024**, *73*, 14044–14049. https://doi.org/10.1109/TVT.2024.3395373.
42. Boyd, S. Convex optimization. *Cambridge UP* **2004**.
43. Nocedal, J.; Wright, S.J. *Numerical optimization*; Springer, 1999.
44. Lindqvist, B.; Mansouri, S.S.; Agha-mohammadi, A.a.; Nikolakopoulos, G. Nonlinear MPC for Collision Avoidance and Control of UAVs With Dynamic Obstacles. *IEEE Robotics and Automation Letters* **2020**, *5*, 6001–6008. https://doi.org/10.1109/LRA.2020.3010730.
45. Mayne, D. Model predictive control theory and design. *Nob Hill Pub, Llc* **1999**.